ROYAL SOCIETY OF CHEMISTRY

PAPER

CrossMark
click for updates

Improving the mechanical stability of zirconium-based metal–organic frameworks by incorporation of acidic modulators†

Ben Van de Voorde,[a] Ivo Stassen,[a] Bart Bueken,[a] Frederik Vermoortele,[a] Dirk De Vos,[a] Rob Ameloot,[a] Jin-Chong Tan[*b] and Thomas D. Bennett[*c]

The ability to retain structural integrity under processing conditions which involve mechanical stress, is essential if metal–organic frameworks (MOFs) are to fulfil their potential as serious candidates for use in gas sorption, separation, catalysis and energy conversion applications. A series of zirconium dicarboxylates, predicted to be amongst the more mechanically robust MOFs, have been found to undergo rapid collapse upon ball-milling, resulting in catastrophic losses of porosity. An inverse relationship between collapse time and framework porosity has been found. Addition of acidic modulator ligands (*e.g.* trifluoroacetic acid) to UiO-66 provided a striking increase in mechanical robustness, the degree of which is inversely related to modulator pK_a. This effect, caused by an increased strength of the zirconium–carboxylate bond, provides an important concept to design microporous hybrid frameworks capable of retaining their structure under harsh processing conditions.

Introduction

Metal–organic frameworks (MOFs) are microporous materials incorporating both organic and inorganic moieties connected in a three-dimensional crystal lattice.[1] Extensive research has been performed on the synthesis and structure of MOFs, with applications proposed in *e.g.* separation, gas storage, sensing and catalysis.[2–6] Despite commercial and industrial applications of MOFs necessitating the retention of structure and associated porosity during shaping or post-synthetic processing of powders by mechanical pelletization, extrusion or sintering (forming a solid mass by heating), their physical properties are not well understood at present.[7,8] The instability of some MOFs has already proven problematic in proof-of-concept practical applications,[9–11] though it has been harnessed in other cases to create novel materials[12,13] and also employed to effect the trapping of harmful species.[14]

The zirconium-containing frameworks UiO-66 and the MIL-140 series (Fig. 1) possess chemical and thermal stabilities surpassing those of many other MOFs, which is ascribed to strong bonds between the carboxylates and high valent Zr.[15,16]

This observation, combined with computational reports of the mechanical stability conferred to UiO-66 by its 12-fold connected rigid $Zr_6O_4(OH)_4$ inorganic building blocks,[15,17] renders them excellent candidates for future industrial applications.

Recent research has, however, suggested that crystal defects (*e.g.* missing linkers[18]) may play a key role in determining mechanical stability, and thus empirical verification of the predicted rigid elastic properties is needed. In the following
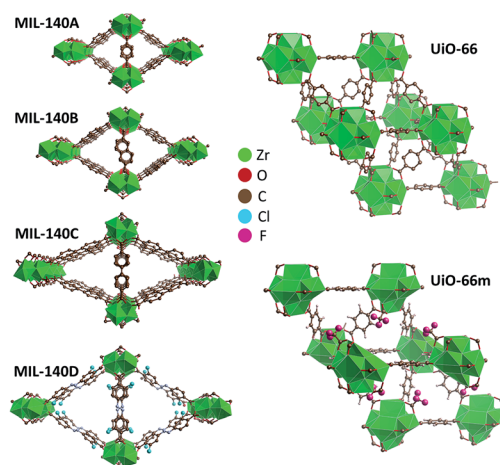
aCentre for Surface Chemistry and Catalysis, KU Leuven, Arenbergpark 23, B-3001 Leuven, Belgium

bDepartment of Engineering Science, University of Oxford, Parks Road, Oxford OX1 3PJ, UK

cDepartment of Materials Science and Metallurgy, University of Cambridge, Cambridge CB3 0FS, UK. E-mail: tdb35@cam.ac.uk

† Electronic supplementary information (ESI) available: X-ray diffraction, thermogravimetric analysis, nitrogen physisorption and pore distribution analysis, scanning electron microscopy images, IR spectroscopy. See DOI: 10.1039/c4ta06396a

Fig. 1 Structures of MIL-140 (A–D), UiO-66 and UiO-66m TFA, with cluster-capping trifluoroacetate molecules.

work, controlled time-dependent ball-milling is used as a high-impact mechanical treatment to gauge stability in shaping operations. We show that, similar to other MOFs,[21] Zr-containing frameworks are highly susceptible to mechanically-induced structural collapse. The inverse relationship between collapse time and micropore volume strongly suggests that the continuing search for higher surface area MOFs[1,22] is unlikely to be accompanied with increases in mechanical strength, and methods for stabilizing these structures must therefore be developed.

Remarkably, addition of different acidic mono-coordinating ligands, which we term modulators, to the structural $Zr_6O_4(OH)_4$ clusters resulted in striking increases in mechanical stability without alteration of the porosity. The stability increase of the modulated UiO-66 variants is enhanced with decreasing modulator pK_a, and is explained by the generation of progressively stronger zirconium–carboxylate bonds through a local electron withdrawing effect. This electronic modulation concept may prove applicable to other MOFs and play a key role in synthesizing structures which are capable of withstanding the mechanical processing necessary for their use in industrial applications.

Experimental

Materials selection and synthesis

The four isoreticular variants of the Zr-oxo chain-based MIL-140 framework selected for this study contain one-dimensional pores with different widths, and were synthesized and evacuated according to previously described literature procedures.[16] The three-dimensionally porous framework UiO-66 was synthesized in a Schott DURAN® pressure plus bottle with a volume of 1 l under static conditions, starting from an equimolar solution of $ZrCl_4$ (3.5 g, 15 mmol) and terephthalic acid (2.5 g, 15 mmol) dissolved in DMF (N,N-dimethylformamide; 155 ml, 2 mol). 1.5 ml of a 36 wt% solution of HCl (17 mmol) was added to the solution and the mixture was placed in a preheated oven at 120 °C for 21 h. The powders were collected *via* centrifugation and thoroughly washed (3 times each) with DMF and ethanol.

A series of UiO-66m X variants (X = TFA – trifluoroacetic acid, ClA – chloroacetic acid, AA – acetic acid) were also studied, being prepared by addition of the acid to the above mixture prior to heating. 10 equivalents (11.5 ml) of CF_3COOH (TFA), 15 equivalents (21.26 ml) of ClH_2COOH (ClA) or 50 equivalents (42.9 ml) of CH_3COOH (AA) were added to the mixture in three separate reactions. The different concentrations of modulator were selected to obtain similar degrees of incorporation of modulator in all samples. For UiO-66m TFA, the addition of the modulator during the synthesis has previously been shown to result in partial replacement of bridging 1,4-benzenedicarboxylate linkers by cluster-capping TFA species.[23] TGA analysis (Fig. S1†) confirmed that comparable quantities of modulator were present in the other modulated samples.

Zeolitic imidazolate framework ZIF-8 [$Zn(mIm)_2$] (mIm: 2-methylimidazolate) was subjected to an identical milling

treatment for comparison, and was activated after being purchased from Sigma Aldrich.

Evaluation of mechanical stability

Analysis of the kinetics of framework collapse was performed by monitoring the evolution of the integral breadth of the last remaining diffraction peak with milling time, in accordance with the method used for analyzing the crystallinity of UiO-66 frameworks under pressure.[16] Collapse times were taken as the point at which no Bragg peaks were remaining.

In all milling treatments, 50 mg of each sample was placed in a 10 ml stainless steel jar along with one 9 mm diameter stainless steel ball. The material was then ball-milled for varying amounts of time in a Retsch MM400 grinder mill operating at 20 Hz. Samples were not placed back into the ball-mill after analysis (*i.e.* 20 minutes of ball-milling was done continuously, rather than four 5 minute intervals), to prevent mass loss during analysis. Temperature increases in previous ball-milling experiments have been observed to be negligible.[24]

Room temperature PXRD data were collected after milling, using a Bruker-AXSD8 diffractometer using $CuK\alpha_1$ (λ = 1.540598 Å) radiation and a LynxEye position sensitive detector in Bragg Brentano parafocusing geometry. Analysis of the data was carried out using the X'Pert HighScore Plus program. Structureless pattern profile refinements of low angle data (2θ = 5–20°) were also carried out using X'Pert HighScore Plus. Refinement of experimental background, cell parameters, W and V parameters and two asymmetry parameters were undertaken. The integral breadth (peak area/peak maximum) of the first diffraction peak at $2\theta \approx 7°$ (the last remaining peak upon amorphization) was used instead of the FWHM, as an anti-scattering knife-edge on the X-ray diffractometer resulted in an increasing background at low-angle. The last remaining diffraction peaks used for profile fitting were the (200), (111) and (011) for MIL-140 frameworks, the UiO-66 variants and ZIF-8 respectively (Fig. S2a–l†).

Characterization of materials

Nitrogen physisorption isotherms were measured at 77 K with a Micromeritics 3Flex surface characterization analyser. Prior to the measurements, the powders (50–80 mg) were outgassed for 4 h at 473 K and 10^{-1} mbar vacuum.

Surface area and pore size distribution calculations were carried out using the 3Flex Version 1.01 program. The BET method was applied on the data points between 0.005 and 0.05 p/p_0. Calculation in this region resulted in both a positive C value and an increasing Rouquerol transform for all samples. External surfaces were calculated with the t-plot method (Harkins and Jura thickness equation; thickness range 3.5–5 Å). Micropore areas were obtained by subtracting the external surface from the BET surface area. Pore-size distributions were calculated with the Tarazona NLDFT model (regularization factor 0.001).

For IR spectroscopy, the samples (1 wt%) were pressed in a KBr pellet and were outgassed in the sample chamber under secondary vacuum (<4 mbar) at room temperature for the

1738 | J. Mater. Chem. A, 2015, 3, 1737–1742

This journal is © The Royal Society of Chemistry 2015

spectra of the 400–800 and 1600–1800 cm^{-1} regions, or at elevated temperatures (50–200 °C) for the 3500–3800 cm^{-1} region. Transmission IR spectra were measured on a FTIR Bruker type IFS 66/v/S equipped with a cryo-detector, with a 4 cm^{-1} resolution.

Thermogravimetric analyses were performed on a TA instruments TQA 500 machine. Measurements were performed by heating the samples at 5 °C min^{-1} under nitrogen.

Scanning electron micrographs were recorded on Au-coated samples using a Philips XL30 FEG microscope.

Results and discussion

Facile, porosity-dependent collapse

Powder X-ray diffraction indicated rapid losses in crystallinity upon milling of the non-modulated frameworks, resulting in loss of Bragg intensity and appearance of broad diffuse scattering, indicating amorphization. For the MIL-140 frameworks, collapse times decreased with increasing linker length, whilst UiO-66 was the least stable Zr-MOF (Table 1). For this series of five Zr-MOFs, this results in an inversely proportional relationship between micropore volume and collapse time (Fig. 2a). The short collapse time of UiO-66 of less than 10 minutes is remarkably similar to that of the 'soft' porous framework ZIF-8, which contains relatively simple ZnN_4 tetrahedral inorganic nodes. Indeed, the comparable pore volumes of the two materials (Table 1) suggest that no significant stabilization against ball-milling is conferred to UiO-66 by the multi-connected nature of its $Zr_6O_4(OH)_4$ building block. This is surprising given the differences between the two structures and recent theoretical studies on UiO-66 suggesting its particularly robust nature.[17]

Low values of the minimum shear modulus, G_{min}, of MOFs have previously been invoked to explain their instability and in particular, the rapid collapse of ZIF-8 ($G_{min} < 1$ GPa).[20] Intriguingly, the considerably higher theoretical shear modulus of UiO-66 (13.75 GPa), which is nearly isotropic ($G_{max}/G_{min} = 1.28$),[17] does not lead to an increase in mechanical stability. One might also expect MIL-140 A ($G_{min} = 0.65$ GPa) to exhibit a low resilience to collapse; however, it is unexpectedly more robust than both UiO-66 and ZIF-8. One possible explanation is that for MIL-140 A, the amorphization process is slowed down by the relatively large predicted G_{max},[19] in combination with short-range
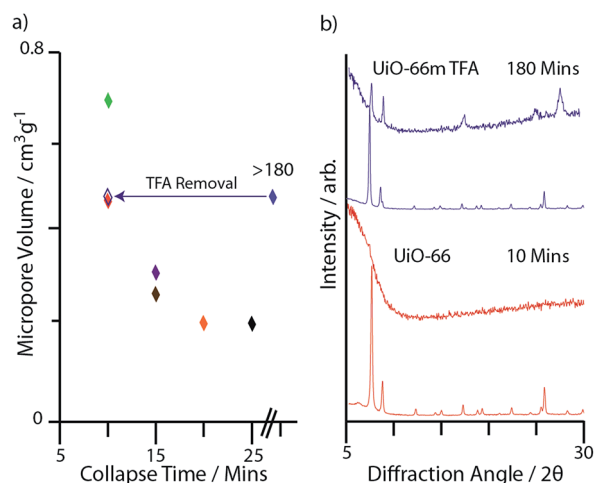

Fig. 2 (a) Collapse times of UiO-66 (red), UiO-66m TFA (blue), ZIF-8 (green) and MIL-140 A–D (purple, brown, orange and black) plotted against micropore volume of the activated material. (b) Diffraction patterns of UiO-66 and UiO-66m TFA before and after milling for 10 and 180 minutes respectively.

dispersive interactions arising from π–π stacking of the aromatic linkers.[16] However, the presence of defects in materials like UiO-66 may also strongly influence the eventual mechanical properties,[18] and this raises the question how materials might be modified to reach their theoretical stabilities.

The reduction in particle size of each sample upon ball-milling was monitored by scanning electron microscopy (SEM). Initial crystallite sizes ranged from 2–10 μm for the MIL-140 series, to <1 μm for the UiO-66 variants (Fig. S3a–g†). Rapid decreases in particle size were noted during the first ten minutes of milling, with no significant further changes. The dissociation between particle size and crystallinity is clearly observed for MIL-140 A–C, which retain crystallinity upon reduction to sub-micron particle sizes (Fig. S2a–c†), and then undergo subsequent loss of long range order (amorphization) with negligible further changes in particle size.

Acidic modulator based framework stabilization

Recently, the incorporation of trifluoroacetic acid in the UiO-66 framework has been reported to assist in the generation of additional Lewis acid sites and to increase the catalytic

Table 1 Structural characteristics for MIL-140 (A–D), UiO-66 without modulator and ZIF-8

Name	Ideal structural formula	Measured micropore volume[a] (cm^3 g^{-1})	Collapse time/min	Minimum and maximum shear moduli G_{min}/G_{max}[b] (GPa)
MIL-140 A	$ZrO[O_2C–C_6H_4–CO_2]$	0.218	20–25	0.65/23.4 (ref. 19)
MIL-140 B	$ZrO[O_2C–C_{10}H_6–CO_2]$	0.214	15–20	
MIL-140 C	$ZrO[O_2C–C_{12}H_8–CO_2]$	0.280	10–15	
MIL-140 D	$ZrO[O_2C–C_{12}H_6Cl_2–CO_2]$	0.322	10–15	
UiO-66	$Zr_6O_4(OH)_4[O_2C–C_6H_4–CO_2]_6$[c]	0.482	5–10	13.75/17.63 (ref. 17)
ZIF-8	$Zn(C_4H_5N_2)_2$	0.694	5–10	0.94/1.33 (ref. 20)

[a] Total pore volume determined at $p/p_0 = 0.9$. [b] Theoretical predictions obtained from density functional theory (DFT)[17,19] except for ZIF-8 (values derived from Brillouin scattering experiments[20]). [c] Based on TGA analysis, the actual formula in this study is $Zr_6O_6(OH)_2[O_2C–C_6H_4–CO_2]_5$. C_6H_4 – benzene, $C_{10}H_6$ – naphthalene, $C_{12}H_8$: 4,4'-biphenyl.

This journal is © The Royal Society of Chemistry 2015

J. Mater. Chem. A, 2015, **3**, 1737–1742 | **1739**

activity.[23] TFA groups partly replace some of the cluster linking benzene dicarboxylate ligands in this material (UiO-66m TFA), leading to a more open framework with a representative formula $Zr_6O_7(OH)[O_2C-C_6H_4-CO_2]_4[CF_3CO_2]$. The TFA : Zr ratio of 10 : 1 used in the literature synthesis results in an average incorporation of one trifluoroacetate (TFA) per cluster as determined by solid state ^{19}F-NMR.[23]

Notably, despite possessing almost the same micropore volume as UiO-66 (0.497 *vs.* 0.492 cm^3 g^{-1}), UiO-66m TFA exhibited remarkable stability upon ball-milling, retaining Bragg diffraction for over 3 hours (Fig. 2b and S2g†). This is in strong contrast to previous studies on the ZIF series, where higher elastic moduli and thus framework rigidity are typically linked to increases in framework density.[25] Upon heating at 350 °C for several hours, TFA molecules are removed from the UiO-66m TFA (Fig. S4a†).[23] Samples treated as such, termed UiO-66mh, were observed to collapse in a similar time (<10 min) as the non-modulated UiO-66 sample (Fig. S2i†), providing evidence for the beneficial effect of the modulator in enhancing the mechanical stability of the framework.

The N$_2$ gas uptake capacities at 77 K of all crystalline and amorphized frameworks (hereby referred as a$_m$MOFs, where the subscript m indicates amorphization by ball-milling) were measured, along with their BET, micropore and external surface areas (Table 2). In the analysis, the partially amorphized UiO-66m TFA after 25 minutes of ball-milling was used, to provide some comparison with the other materials.

The type I isotherms for the crystalline phases (Fig. S5a†) are in broad agreement with those previously published.[16] Unsurprisingly, overall BET surfaces decrease markedly upon amorphization in each case, accompanied by a striking decrease to negligible micropore volumes (Table 2). This was not the case for UiO-66m TFA, where N$_2$ physisorption analysis (Fig. 3) indicated retention of *ca.* 20% of micropore volume upon ball-milling.

Pore size distributional analysis of crystalline UiO-66 (Fig. S5b–g†) illustrated not only the presence of the expected small tetrahedral and large octahedral cages; even larger cage and channel dimensions were found. We ascribe this to the now well-documented phenomenon of linker deficiency, resulting in the merger of neighbouring cages.[18,23,26,27] TGA analysis showed ~2 missing linkers per cluster for UiO-66. This phenomenon is even more pronounced for UiO-66m TFA (Fig. 3), in which partial substitution of terephthalate linkers by incorporated
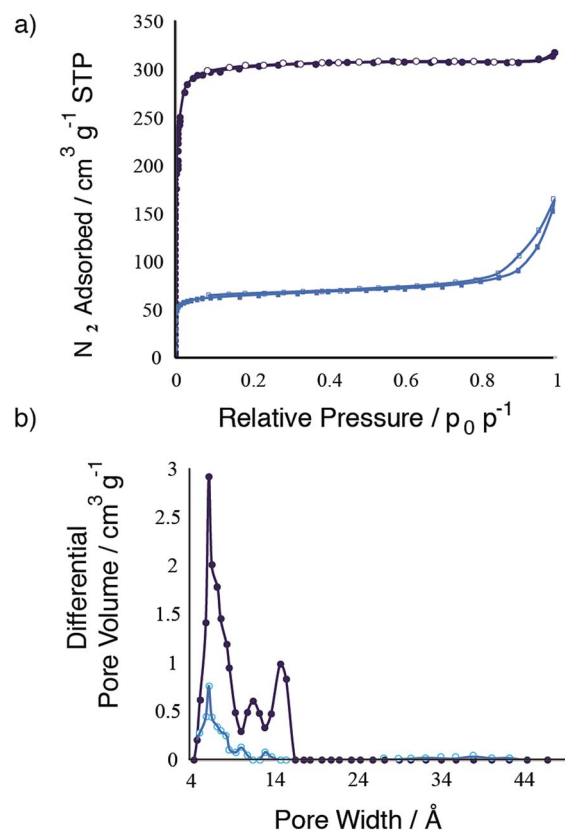

Fig. 3 (a) Nitrogen sorption isotherms at 77 K for UiO-66m TFA (dark blue) and UiO-66m TFA after 25 minutes of ball-milling (light blue). Open symbols – desorption, closed symbols – adsorption. (b) Pore size distributional analysis for crystalline (dark blue) and partially amorphized (light blue) UiO-66m TFA after 25 min milling.

TFA molecules leaves only 8 bicipital linkers around the cluster, rather than the maximum of 12. After partial amorphization, the residual microporosity largely corresponds to the smallest pore diameters in the starting material, indicating that the largest pores in the starting UiO-66m TFA suffer the most drastic decreases in associated volume upon milling.

Structural changes upon milling

Samples of a$_m$MIL-140 A–D were observed to lose 5–10 wt% of water between 50 and 150 °C before thermal degradation at 500 °C (Fig. S6a†). This is in contrast to the negligible water loss for the crystalline frameworks, which are hydrophobic. The increased hydrophilicity upon amorphization is in agreement with an increase in the free carboxylic acid IR stretching vibration at ~1700 cm^{-1}, and the detection of strongly bound water for amorphized MIL-140 A (Fig. S7a†).

Markedly different behavior is observed in the cases of crystalline UiO-66 and UiO-66m TFA, which show two weight loss steps corresponding to release of physisorbed H$_2$O at 100 °C, and dehydroxylation of the Zr clusters around 250 °C. An additional step is present in the TGA for the latter at *ca.* 300 °C, corresponding to the loss of trifluoroacetate molecules, in agreement with existing literature.[23] Initial weight loss from

Table 2 Surface areas for crystalline and amorphized (in brackets) samples

Sample	BET (m^2 g^{-1})	Micropore (m^2 g^{-1})	External area (m^2 g^{-1})
MIL-140 A	484 (16)	425 (3)	59 (13)
MIL-140 B	483 (41)	405 (29)	78 (13)
MIL-140 C	682 (23)	601 (15)	81 (7)
MIL-140 D	545 (6)	472 (1)	73 (6)
UiO-66	1129 (13)	1003 (3)	126 (10)
UiO-66m TFA	1249 (254)	1152 (203)	97 (51)
ZIF-8	2048 (43)	2382 (10)	23 (33)

1740 | *J. Mater. Chem. A*, 2015, **3**, 1737–1742

This journal is © The Royal Society of Chemistry 2015

Table 3 Difference in collapse time for various modulated and non-modulated UiO-66 variants, along with the pK_a of the modulator (or ligand in case of the non-modulated UiO-66)

	UiO-66m TFA	UiO-66m ClA	UiO-66mh[a]	UiO-66	UiO-66m AA
pK_a	∼0	2.86	—	3.51, 4.82	4.76
Collapse time (min)	>180	10	5–10	5–10	<5

[a] UiO-66m TFA heated at 350 °C, in order to remove the TFA from the Zr-cluster.

a_mUiO-66 and a_mUiO-66m TFA is much lower, reflecting a decrease in porosity relative to their parent crystalline frameworks. As the amorphization of UiO-66 is complete after 10 minutes of milling, no further increase in free carboxylate stretch can be detected even after prolonged milling (10–20 minutes).

To understand the remarkable increase in mechanical stability of UiO-66m TFA, samples of UiO-66 modulated with acetic acid (UiO-66m AA) and chloroacetic acid (UiO-66m ClA)[23] were also analysed (Fig. S2j and k†). Collapse times were found to be inversely related to the pK_a value of the modulator or ligand, with UiO-66m TFA remaining the most stable sample (Table 3). Analysis of the increase in integral breadth of the last remaining diffraction peaks with milling time (Fig. 4) confirmed the intermediate stability of the sample modulated with chloroacetic acid.

The stabilization is ascribed to an electronic effect on the Zr–carboxylate bonds by the incorporation of the modulator, since its removal from UiO-66m TFA results in shorter collapse times. This can be understood as a local electron withdrawing effect, which increases the positive partial charge on the Zr^{4+} atom and resulting in a stronger ionic Zr–carboxylate bond.[28,29]

Experimental evidence for the effect is directly provided by IR spectroscopy (Fig. 5). The band at *ca.* 744 cm^{-1} (assigned to in phase C–H bending of the terephthalate) remains invariable for the different modulated materials. The band around 545–
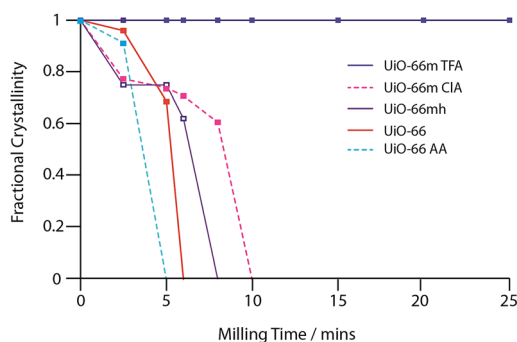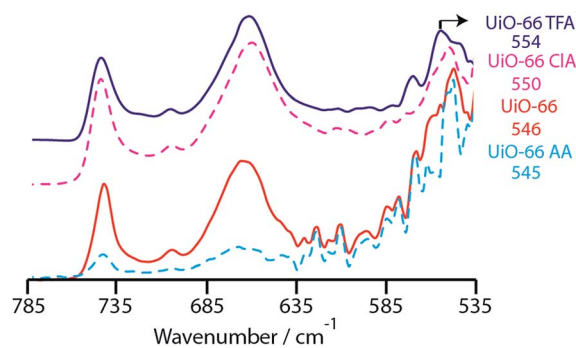

Fig. 5 IR spectra following the Zr–OC asymmetric stretching vibration of the modulated UiO-66 samples.

555 cm^{-1} is assigned to the Zr–(OC) asymmetric stretching vibration,[26] and moves to progressively higher wavenumber with decreasing modulator pK_a, implying a strengthening of the bond. The position of this band in UiO-66m AA and UiO-66 is consistent with the rapid collapse of these materials. Note that the symmetric stretching is not observed in hydroxylated UiO-66 samples.[26]

The vibration at 663 cm^{-1} is assigned to a vibration of the hexanuclear cluster, in line with its absence from the IR spectra of MIL-140 A. The increased stability of UiO-66 TFA is also evidenced by the persistence of this characteristic vibration, even after 25 minutes of milling. This is in stark contrast to UiO-66 where the feature broadens and disappears before this time (Fig. S7b and c†).

Conclusions

Zr-containing MOFs, predicted to be among the most physically robust of this family of 'soft' porous materials, undergo rapid collapse under ball-milling. This collapse is accompanied by chemical changes (*e.g.*, complete destruction of the clusters) beyond the simple decrease down to X-ray amorphous particle sizes, which, along with prior results for ZIFs,[21] indicates that this is a general phenomenon. The unfortunate, yet intuitive result that frameworks of higher porosities[30] undergo faster and more comprehensive structural collapse has important consequences for MOF mechanical processing. Addition of modulators like chloroacetic and particularly trifluoroacetic acid to UiO-66 synthesis results in striking increases in physical stability under ball-milling, despite generating more materials of almost identical porosity. In the case of the latter, TFA modulated framework, porosity is retained for at least a 10 times longer duration. A relationship between modulator pK_a and material stability has been established. This is a promising concept to create 'super-strong' hybrid frameworks, capable of resisting the pressures or stresses involved in post-synthesis processing and shaping.

Fig. 4 Analysis of the crystallinity for various modulated UiO-66 samples as a function of milling time (TFA = trifluoroacetic acid; ClA = chloroacetic acid; AA = acetic acid, mh = modulated removed by heating). Fractional crystallinity is calculated from starting integral breadth/integral breadth at time *t*.

This journal is © The Royal Society of Chemistry 2015

J. Mater. Chem. A, 2015, **3**, 1737–1742 | **1741**

Notes and references

1 H. Furukawa, K. E. Cordova, M. O'Keeffe and O. M. Yaghi, *Science*, 2013, **341**, 974–986.

2 F. Vermoortele, M. Vandichel, B. Van de Voorde, R. Ameloot, M. Waroquier, V. Van Speybroeck and D. E. De Vos, *Angew. Chem., Int. Ed.*, 2012, **51**, 4887–4890.

3 J. R. Li, R. J. Kuppler and H. C. Zhou, *Chem. Soc. Rev.*, 2009, **38**, 1477–1504.

4 T. D. Bennett, P. J. Saines, D. A. Keen, J. C. Tan and A. K. Cheetham, *Chem.–Eur. J.*, 2013, **19**, 7049–7055.

5 G. Lu and J. T. Hupp, *J. Am. Chem. Soc.*, 2010, **132**, 7832–7833.

6 B. Van de Voorde, B. Bueken, J. Denayer and D. De Vos, *Chem. Soc. Rev.*, 2014, 5766–5788.

7 J. C. Tan and A. K. Cheetham, *Chem. Soc. Rev.*, 2011, **40**, 1059–1080.

8 T. D. Bennett and A. K. Cheetham, *Acc. Chem. Res.*, 2014, **47**, 1555–1562.

9 D. Bazer-Bachi, L. Assié, V. Lecocq, B. Harbuzaru and V. Falk, *Powder Technol.*, 2014, **255**, 52–59.

10 G. W. Peterson, J. B. DeCoste, T. G. Glover, Y. G. Huang, H. Jasuja and K. S. Walton, *Microporous Mesoporous Mater.*, 2013, **179**, 48–53.

11 E. Proietti, F. Jaouen, M. Lefevre, N. Larouche, J. Tian, J. Herranz and J. P. Dodelet, *Nat. Commun.*, 2011, **2**, 416.

12 T. D. Bennett, A. L. Goodwin, M. T. Dove, D. A. Keen, M. G. Tucker, E. R. Barney, A. K. Soper, E. G. Bithell, J. C. Tan and A. K. Cheetham, *Phys. Rev. Lett.*, 2010, **104**.

13 T. D. Bennett, D. A. Keen, J. C. Tan, E. R. Barney, A. L. Goodwin and A. K. Cheetham, *Angew. Chem., Int. Ed.*, 2011, **50**, 3067–3071.

14 K. W. Chapman, D. F. Sava, G. J. Halder, P. J. Chupas and T. M. Nenoff, *J. Am. Chem. Soc.*, 2011, **133**, 18583–18585.

15 J. H. Cavka, S. Jakobsen, U. Olsbye, N. Guillou, C. Lamberti, S. Bordiga and K. P. Lillerud, *J. Am. Chem. Soc.*, 2008, **130**, 13850–13851.

16 V. Guillerm, F. Ragon, M. Dan-Hardi, T. Devic, M. Vishnuvarthan, B. Campo, A. Vimont, G. Clet, Q. Yang, G. Maurin, G. Férey, A. Vittadini, S. Gross and C. Serre, *Angew. Chem., Int. Ed.*, 2012, **51**, 9267–9271.

17 H. Wu, T. Yildirim and W. Zhou, *J. Phys. Chem. Lett.*, 2013, **4**, 925–930.

18 H. Wu, Y. S. Chua, V. Krungleviciute, M. Tyagi, P. Chen, T. Yildirim and W. Zhou, *J. Am. Chem. Soc.*, 2013, **135**, 10525–10532.

19 A. U. Ortiz, A. Boutin, A. H. Fuchs and F. X. Coudert, *J. Chem. Phys.*, 2013, **138**, 174703.

20 J. C. Tan, B. Civalleri, C. C. Lin, L. Valenzano, R. Galvelis, P. F. Chen, T. D. Bennett, C. Mellot-Draznieks, C. M. Zicovich-Wilson and A. K. Cheetham, *Phys. Rev. Lett.*, 2012, **108**, 095502.

21 T. D. Bennett, S. Cao, J. C. Tan, D. A. Keen, E. G. Bithell, P. J. Beldon, T. Friscic and A. K. Cheetham, *J. Am. Chem. Soc.*, 2011, **133**, 14546–14549.

22 H. K. Chae, D. Y. Siberio-Pérez, J. Kim, Y. Go, M. Eddaoudi, A. J. Matzger, M. O'Keeffe and O. Yaghi, *Nature*, 2004, **427**, 523–527.

23 F. Vermoortele, B. Bueken, G. Le Bars, B. Van de Voorde, M. Vandichel, K. Houthoofd, A. Vimont, M. Daturi, M. Waroquier, V. Van Speybroeck, C. Kirschhock and D. E. De Vos, *J. Am. Chem. Soc.*, 2013, **135**, 11465–11468.

24 P. J. Beldon, L. Fabian, R. S. Stein, A. Thirumurugan, A. K. Cheetham and T. Friscic, *Angew. Chem., Int. Ed.*, 2010, **49**, 9640–9643.

25 J. C. Tan, T. D. Bennett and A. K. Cheetham, *Proc. Natl. Acad. Sci. U. S. A.*, 2010, **107**, 9938–9943.

26 L. Valenzano, B. Civalleri, S. Chavan, S. Bordiga, M. H. Nilsen, S. Jakobsen, K. P. Lillerud and C. Lamberti, *Chem. Mater.*, 2011, **23**, 1700–1718.

27 M. J. Katz, Z. J. Brown, Y. J. Colon, P. W. Siu, K. A. Scheidt, R. Q. Snurr, J. T. Hupp and O. K. Farha, *Chem. Commun.*, 2013, **49**, 9449–9451.

28 L. M. Yang, E. D. Ganz, S. Svelle and M. Tilset, *J. Mater. Chem. C*, 2014, **2**, 7111–7125.

29 A. Nimmermark, L. Ohrstrom and J. Reedijk, *Z. Kristallogr.*, 2013, **228**, 311–317.

30 R. L. Martin and M. Haranczyk, *Chem. Sci.*, 2013, **4**, 1781–1785.

1742 | *J. Mater. Chem. A*, 2015, **3**, 1737–1742

This journal is © The Royal Society of Chemistry 2015